

Mechanical Properties of Alternating Copolymers of Acrylonitrile and Butadiene

J. FURUKAWA and A. NISHIOKA,* *Department of Synthetic Chemistry, Kyoto University, Kyoto, Japan*

Synopsis

The alternating copolymer was prepared from butadiene (BD) and acrylonitrile (AN) with ethylaluminum dichloride as a complexing agent and with vanadyl chloride as a co-catalyst, and was investigated to explain effects of composition and sequence distribution on the physical properties, especially the viscoelastic properties and the ultimate mechanical properties. In the unvulcanized state, the viscoelastic properties of the alternating rubber is not essentially different from the random one, except for a slight difference in the relaxation spectra. However, the vulcanized rubbers show different shift factors. The latter depends upon the glass transition temperature (T_g). Since the alternating copolymer possesses a T_g lower than the random one, the nature of the alternating copolymer corresponds to that of the random copolymer having an AN content of 40%. The difference in dynamic properties can be expressed with the different shift factors. In the isofree-volume state or at the temperature $T_g + 25^\circ\text{C}$, the rubbers having various acrylonitrile contents and various degrees of alternation exhibit almost the same dynamic properties. However, the strain at break of the alternating rubber is higher than that of the random one. The temperature of maximum strain increases with increasing degree of alternation. The alternating rubber shows higher stress at break than the random one. The stiffness of the chain of the alternating copolymer is smaller than the random copolymer; in other words, the molecular chain of the former is more flexible than the latter. It can be said that the alternating copolymer is an excellent rubber having high tensile strength and elongation at break.

INTRODUCTION

The alternating copolymer of AN and BD, a new class of elastomer of practical and theoretical interest, was originally prepared by Furukawa and Iseda.¹ This novel copolymer has a unique and desirable combination of properties,³⁻⁵ but the quantitative aspects of the change of the microstructure have not been explored extensively. The effect of microstructure on physical properties has long been a research goal. A systematic examination of the effect of the composition and the sequence distribution on the physical properties of the copolymer is desirable. The advent of controlled sequence regularity copolymerization, through a suitable catalyst, provides a mean to synthesize the copolymer of the desired sequence distribution.

* Present address: Japan Synthetic Rubber Co., Research Center, Ikuta, Kawasaki, Japan.

In the previous paper, we have discussed the glass transition temperature of the alternating copolymer of acrylonitrile and butadiene.⁵

In this study, a series of AN-BD copolymers were prepared by conventional radical emulsion polymerization and by organometallic catalyst polymerization,^{1,2} in order to obtain the copolymer of various degrees of alternation. The effects of the composition and the sequence regularity on the mechanical properties were investigated, especially on the viscoelastic and ultimate mechanical properties.

EXPERIMENTAL

Materials. Compositions, T_g , and Mooney viscosities of the copolymers used are listed in Table I. Samples R-1 to R-5 are a series of commercially available copolymers of various AN content. They were prepared by the conventional emulsion polymerization technique, and their commercial names are JSR N240S, N230S, N220S, Hycar 1000 \times 88, and Hycar 1000 \times 132, respectively. Samples R-6 and R-7 were prepared in our laboratory, by the method of radical polymerization, the former in emulsion and the latter in solution. Samples A-1 to A-4 are equimolar copolymers of various sequence distribution which were prepared with ethylaluminum dichloride as complexing agent and with vanadyl chloride as cocatalyst.

TABLE I
Compositions and Properties of Acrylonitrile-Butadiene Rubbers

Sample no.	AN content, ^a mole-%	R^b	ML_{1+4}	T_g^c , °C
R-1	27.3	—	59	-45
R-2	35.5	—	66	-36
R-3	41.4	78	96	-26
R-4	42.3	—	94	-27
R-5	49.9	81	47	-23
R-6	51.0	—	165	-17
R-7	45.0	—	60	-28
A-1	48.5	93	200	-25
A-2	50.0	83	40	-18
A-3	50.8	82	53	-15
A-4	49.5	82	75	-8

^a Determined from C.H.N. elemental analysis.

^b Determined from NMR spectrum analysis.⁵

^c Determined from DSC measurement.⁵

Preparation and Treatment of Pure Gum Vulcanizates. Vulcanizates were prepared in the form of 15-cm square sheets, 1 mm thick. The rubber (100) parts by weight zinc oxide (5.0), stearic acid (1.0), antioxidant 2246 [2,2'-methylene-bis(α -methyl-6-*tert*-butylphenol)] (1.0), and varied amounts (0.5-1.5) of sulfur and dibenzothiazyl disulfide were mixed on an open roll and vulcanized in a steam-heated press for 40 or 60 min at 150°C.

Precisely weighed samples of the vulcanizates were immersed in chloro-

form for two days at 25°C to attain equilibrium swelling. The swollen samples were weighed after removal of superfluous swelling agent and dried under vacuum to constant weight. The volume fraction V_r of rubber in the swollen sample was calculated with respect to the rubber excluded with inorganic ingredients. Here, it is assumed that no extra volume contraction occurs in the swollen system.

Stress Relaxation of Green Rubber. Relaxation modulus $E(t)$ in the rubbery region was measured with Pochettino-type relaxometer at temperatures between 20° and 100°C. The relaxation spectrum $H\tau(\tau)$ was obtained from the relaxation modulus using the third approximation method of Yasuda and Ninomiya⁶ and the modified method of Tosaki.⁷

Mooney-Rivlin Plot. The values of C_1 and C_2 , the parameters of the Mooney-Rivlin equation^{8,9} were obtained according to the method described by Maekawa and co-workers.¹⁰ Isochronal stress data were obtained for each strain at a fixed time of 20 min from the tensile stress relaxation measurements at 30°C using a ring-shaped vulcanized specimen.

Dynamic and Static Viscoelasticity. The various relaxation functions for the gum vulcanizates were obtained by dynamic and static measurements. The dynamic data were obtained with a viscoelastic spectrometer¹¹ for a ribbon-shaped specimen of 6.0-cm length, 0.5-cm width, and 0.2-cm thickness at temperatures between -40° and 120°C at frequencies of 1 to 70 cps. The static data were obtained from the stress relaxation experiments for a ribbon-shaped specimens of the same dimensions as mentioned above with an autograph in the temperature range 20° to 100°C and at time of 1 to 1000 sec.

Ultimate Properties. The ultimate strain and stress were recorded on an autograph at a constant extension rate of 0.0417 sec⁻¹ in the temperature range from -60° to 120°C. The ring-shaped samples were tested, four specimens of the same size were usually elongated at the same time at a temperature, and the maximum values were employed as stress and strain.

RESULTS AND DISCUSSION

Relaxation Properties of Green Rubber

The relaxation modulus master curves of the alternating rubber show no unusual features and do not differ qualitatively from similar runs on the other rubber materials, except for different slopes as shown in Figures 1 and 2. The same occurs in the relaxation spectra $H(\tau)$, as shown in Figures 3 and 4.

The Mooney viscosity is proportional to the shear stress near a steady flow at a rate of shear of the order of unity. Since the shear stress in a steady flow is given as a product of the steady-flow viscosity and the rate of shear, Ninomiya and Yasuda¹² have correlated the Mooney viscosity with the relaxation spectrum of a sample after a few appropriate approximations,

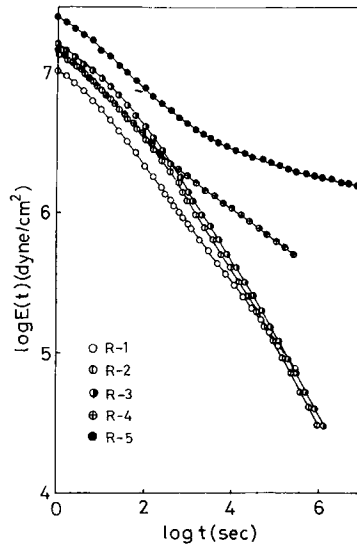


Fig. 1. Master curves of relaxation modulus for uncured radical-type copolymers.

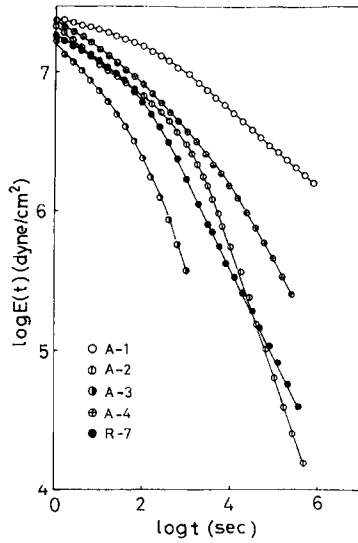


Fig. 2. Master curves of relaxation modulus for uncured alternating-type copolymers.

$$ML_{1+4} = (\pi \cdot \bar{b} \cdot \bar{C} / 2k_s) H(\tau) \Big|_{\tau = \bar{C} / \dot{\gamma}} \quad (1)$$

where ML_{1+4} denotes the Mooney viscosity expressed in Mooney units; k_s is a conversion factor between the torque measured in Mooney units and the shear stress in dynes/cm², whose value was found to be 2×10^4 dynes/cm²/Mooney unit; $\dot{\gamma}$ is the average rate of shear and was found to be 1.25 sec^{-1} ; and \bar{b} and \bar{C} are the empirical parameters which vary only

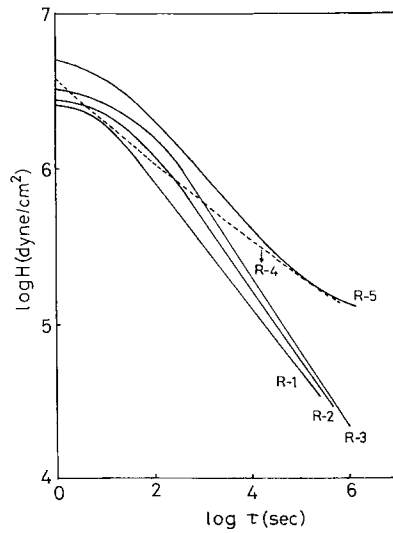


Fig. 3. Relaxation spectra for uncured radical-type copolymers.

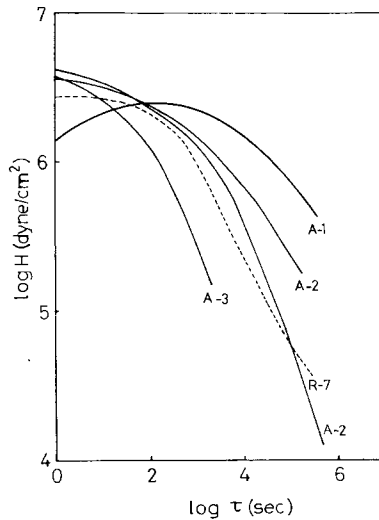


Fig. 4. Relaxation spectra for uncured alternating-type copolymers.

slightly for different rubbers, filler level, etc. Average values for \bar{b} and \bar{C} were found to be 1.3 and 4.2, respectively. As Figure 5 illustrates, the values of ML_{1+4} calculated from eq. (1) agree roughly with those measured for samples used in this work in a log-log graph. Thus, it may be said that the difference in the Mooney viscosity for both types of copolymer is simply correlated with the difference in their shapes of the relaxation spectrum.

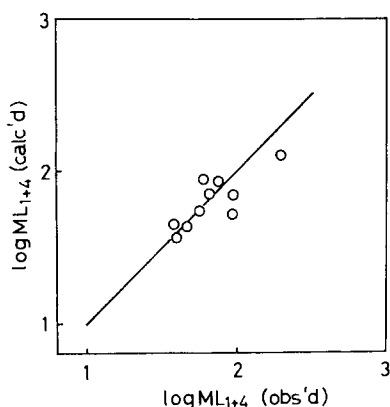


Fig. 5. Mooney viscosities, experimentally obtained and calculated from relaxation spectrum.

Crosslink Density

Mechanical properties of the vulcanized rubber strongly depend on the crosslink density, rather than on the rheological property of the raw rubber. Consequently, it is important to estimate the crosslink density of the samples in question.

The isochronal stress-strain data obtained from the stress relaxation at an elongation up to about 120% fit fairly well into the Mooney-Rivlin equation:^{8,9}

$$S = 2C_1\left(\alpha^2 - \frac{1}{\alpha}\right) + 2C_2\left(\alpha - \frac{1}{\alpha^2}\right) \quad (2)$$

where α is the extension ratio and S stands for the true stress. Only the first term in this equation seems to be physically understood in the theory of rubber elasticity. The Mooney-Rivlin equation seems to hold from a linear relationship between $S/(\alpha^2 - 1/\alpha)$ and $1/\alpha$, as shown in Figure 6. According to the theory of rubber elasticity, a modulus denoted as $2C_1$ is related to the crosslink density, ν , in the form

$$2C_1 = S\left(\alpha^2 - \frac{1}{\alpha}\right) = \nu RT. \quad (3)$$

The crosslink density thus estimated for each gum vulcanizate is plotted against the equilibrium volume ratio of swelling, V_r , as illustrated in Figure 7. The swelling behavior is generally expressed by the Flory-Rehner equation,^{13,14}

$$\nu = -\frac{V_r + \mu V_r^2 + \ln(1 - V_r)}{V_0(V_r^{1/3} - V_r/2)}, \quad (4)$$

where V_0 is the molar volume of the solvent and μ is an interaction pa-

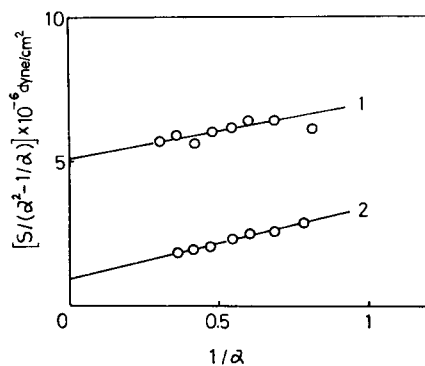


Fig. 6. Mooney-Rivlin plots for a sample: (1) cured by sulfur, 1.5 parts; (2) cured by sulfur, 0.5 parts.

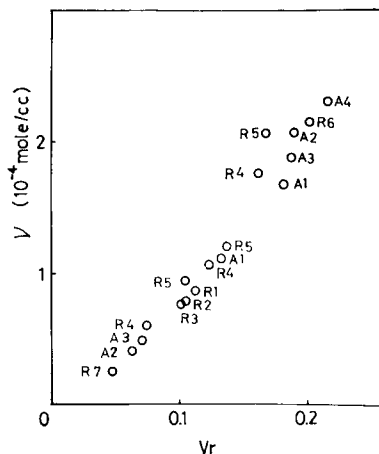


Fig. 7. Volume fraction of rubber in swollen network (V_r) vs. crosslink density (ν).

parameter in a given polymer-solvent system. Substitution of data on ν and V_r into eq. (4) gives

$$\mu = 0.2 + 0.8V_r \tag{5}$$

The estimated value of μ in NBR-chloroform system appeared practically unchanged irrespective of the composition and the microstructure in the ranges examined.

Shift Factor

The isothermal mechanical data for each sample were obtained at various temperatures between -40° and 120°C either by dynamic or static measurements. According to the usual method, a master curve was constructed for each sample. An example of the master curve thus obtained is illustrated in Figure 8, where the complex modulus in extension,

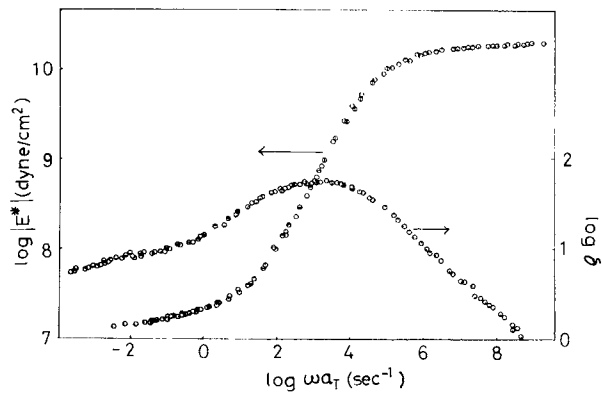


Fig. 8. Master curves of $|E^*|$ and δ for a sample ($T_0 = 25^\circ\text{C}$).

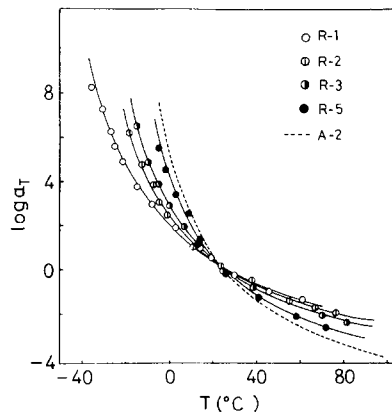


Fig. 9. Temperature dependence of $\log a_T$ for radical-type copolymers ($T_0 = 25^\circ\text{C}$).

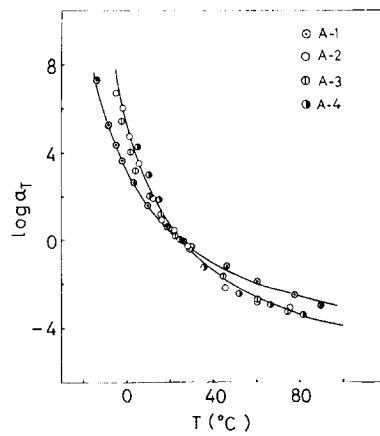


Fig. 10. Temperature dependence of $\log a_T$ for alternating-type copolymers ($T_0 = 25^\circ\text{C}$).

$|E^*|$, and the phase angle δ are plotted double-logarithmically against the angular frequency ω . The shift factor a_T , obtained therefrom for various samples, is shown in Figures 9 and 10 where 25°C was chosen as the reference temperature for all cases. The temperature dependence of the shift factor was then analyzed in terms of the WLF equation

$$\log a_T = -C_1^0(T - T_0)/(C_2^0 + T - T_0) \quad (6)$$

where T represents the temperature and C_1^0 , C_2^0 , and T_0 are the temperature-independent parameters, the last one representing the reference temperature. The experimental data were found to fit the WLF equation as shown in Figures 9 and 10, where the relation given by eq. (6) is shown by a solid curve for each sample. The WLF parameters C_1^0 and C_2^0 are further related to the free volume of the system and its thermal expansion coefficient. They are listed in Table II. The values of T_g obtained from viscoelastic data almost agree with those determined from the DSC measurements.⁵ Since the thermal coefficient of the free volume is known to be fairly insensitive to the change in the internal and/or chemical structures of polymers, the differences in the $\log a_T$ curves among those samples may be mainly attributed to the change in free volume. Therefore, it may be generally expected to obtain a single composite plot irrespective of the internal structure of the samples, if the data on $\log a_T$ are taken at an isofree-volume state. Since the value of the fractional free volume of a polymer is known to come around 0.025 at its glass temperature T_g , irrespective of the species of the polymer, T_g or $T_g + A$ (A being constant) may be used for each sample as the reference temperature for the comparison at an isofree-volume state. The shift factors thus obtained for various samples were found to simply correlate with the reference temperatures, as shown in Figure 11.

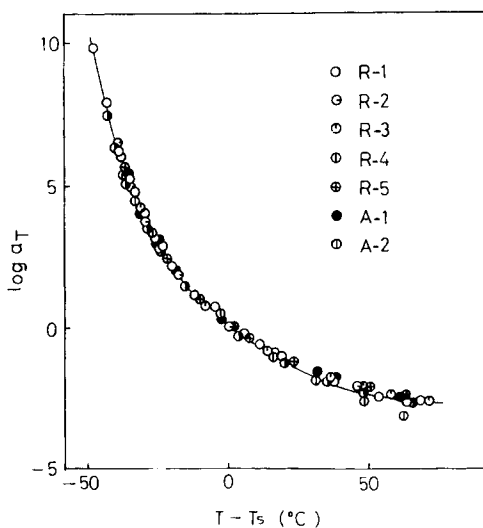


Fig. 11. Temperature dependence of $\log a_T$ reduced to isofree-volume state ($T_s = T_g + 50^\circ\text{C}$).

TABLE II
 WLF Parameters for Various Polymer Systems

Sample no.	$T_g, ^\circ\text{C}$	C_1^0	C_2^0	$C_1^0 \times C_2^0$
R-1	-42	9.3	58.7	547
R-2	-31	7.6	53.3	405
R-3	-26	8.3	49.0	405
R-4	-23	9.2	99.1	913
R-5	-16	6.2	64.5	399
R-6	-14	7.6	70.3	539
A-1	-22	7.5	56.1	412
A-2	-10	7.4	55.9	416
A-3	-12	7.5	62.3	467
A-4	-8	8.6	66.0	565

Linear Viscoelastic Functions

From the master curves of $|E^*|$ and δ for each sample, the real and the imaginary parts of the complex modulus in extension, denoted respectively as $E'(\omega)$ and $E''(\omega)$, can be calculated as a function of ω . Further, the relaxation modulus $E(t)$, as well as the relaxation spectrum $H(\tau)$, may be estimated therefrom by means of certain approximation methods. Typical data on these linear viscoelastic functions are shown in a double-logarithmic form in Figures 12 to 15.

It is a generally accepted fact that the crosslinking has little effect on the linear viscoelastic behavior of polymers in the transition region if the crosslinking density is sufficiently small like that used in this work. The transition region of any viscoelastic function on the logarithmic time scale is known to be primarily related to the average monomeric friction coefficient of the sample, and this coefficient is influenced largely by the amount of the fractional free volume in the system. Hence, the spread of the transition regions appearing in Figures 12 to 15 may be largely attributed to the variety of T_g among the samples. Figure 16 compares the plots of $\log \tan \delta$ versus $\log \omega$ at an isofree-volume state, i.e., $v_f = 0.05$, for each sample. Although all curves come close to each other in Figure 16 as compared with those in Figure 15, there still remain small but significant differences in the positions of the curves.

The monomeric friction coefficient depends also on some monomeric molecular characteristics such as the monomeric molecular weight M_0 and the root-mean-square end-to-end distance per square root of the number of monomer units, a .¹⁵ If the average is taken for those quantities in the case of copolymers, we may say, regardless of the way of averaging, that the value of M_0 remains fairly unchanged, whereas that of a decreases appreciably as the AN content increases in the sample. This leads us to an expectation that the transition region would be shifted toward the longer time scale region as the amount of the acrylonitrile increases in the copolymer system, provided that the amount of v_f is kept unchanged.

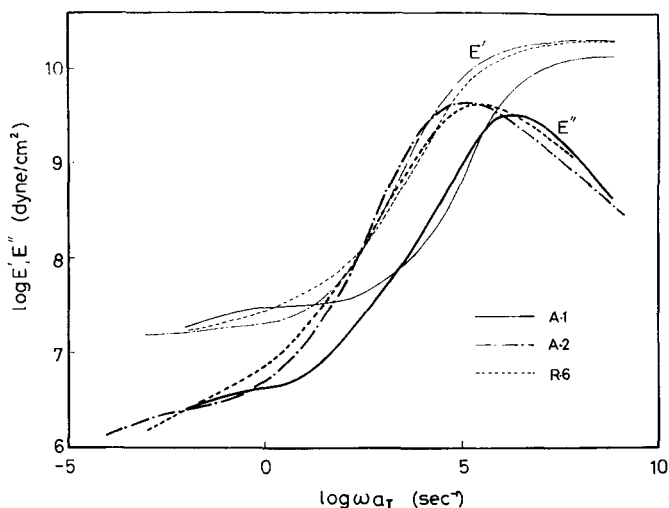


Fig. 12. Master curves of $\log E'$ and $\log E''$ ($T_0 = 25^\circ\text{C}$).

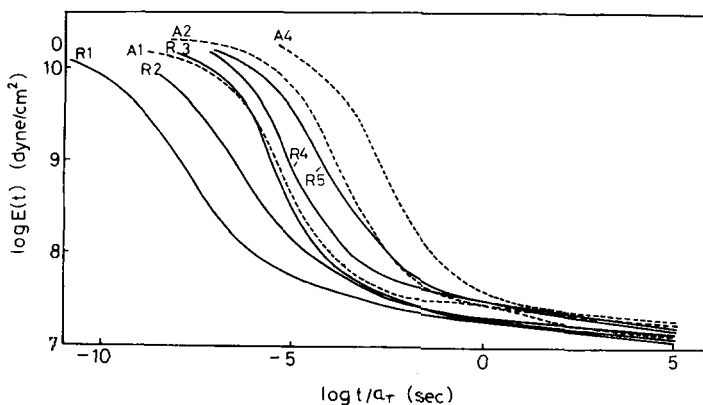
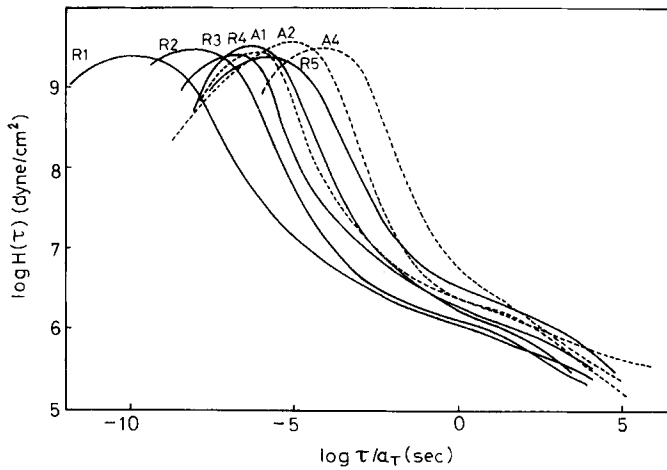
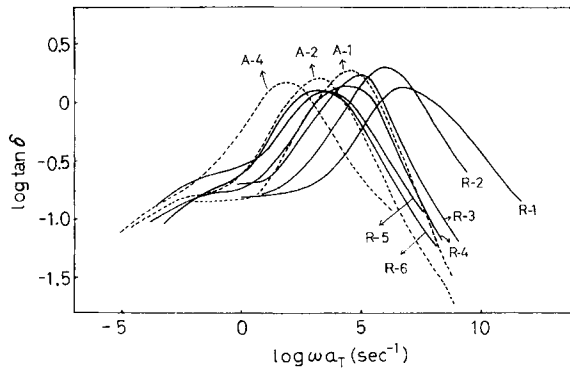


Fig. 13. Master curves of relaxation modulus ($T_0 = 25^\circ\text{C}$).

The frequency at which the principal maximum is reached in the master curve of the loss tangent, which is hereby denoted as $(\omega a_T)_{\max}$, was taken as the measure for the position of the transition region for each sample. Then, $\log(\omega a_T)_{\max}$ obtained at an isofree-volume state for each sample is plotted against its AN content in Figure 17. The value of $\log(\omega a_T)_{\max}$ decreases linearly with increasing AN content, which conforms to the above expectation.

As seen in Figures 12 to 15, the shapes of those linear viscoelastic functions resemble each other in those samples tested, and thus it may be said that the difference in the microstructure in question would have no substantial effect on the linear viscoelastic properties, except for the change in the monomeric friction coefficient in the system.

Fig. 14. Relaxation spectra ($T_0 = 25^\circ\text{C}$).Fig. 15. $\tan \delta$ ($T_0 = 25^\circ\text{C}$).

Ultimate Mechanical Properties

According to the theory proposed recently,¹⁶ the material speciality of the failure behavior of vulcanized rubbers may generally be described by the strain-at-break versus temperature diagram obtained at a certain fixed rate of extension. Figure 18 shows some examples of the diagram obtained in this work.

The strain-at-break versus temperature diagram was found to be generally characterized by five material parameters, including the glass temperature T_g . Since the other two parameters, denoted therein as B_h and B_l , are known to be essentially represented by the linear viscoelastic properties of the sample, the parameters necessary to be investigated here in connection with the internal structure of the sample are the maximum value of the strain at break, $(\gamma_b)_{\max}$, and the temperature, T_{\max} , at which $(\gamma_b)_{\max}$ is reached in the diagram.

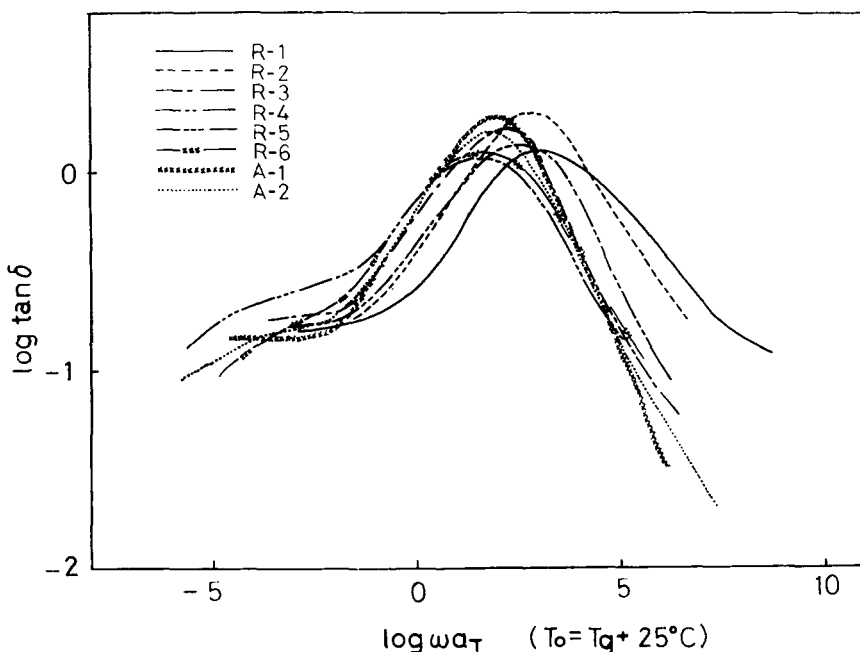


Fig. 16. $\tan \delta$ after reduction to isofree-volume state.

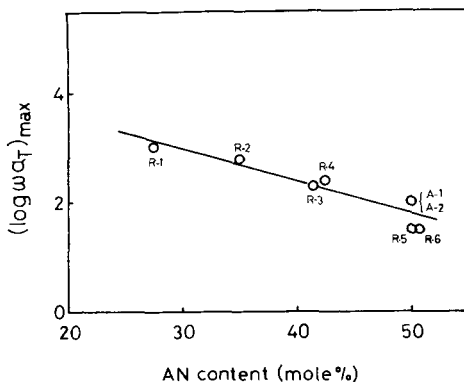


Fig. 17. $(\log \omega a_T)_{\max}$ vs. AN content at isofree-volume state ($T_0 = T_g + 25^\circ\text{C}$).

In Figure 19, $(\lambda_b)_{\max} [= 1 + (\gamma_b)_{\max}]$ is plotted against the AN content of the sample, the crosslink density of each sample being selected around a value of 1×10^{-4} mole/cc. In this figure, it appears that $(\lambda_b)_{\max}$ decreases with the AN-content but increases with the degree of alternation.

For $(\lambda_b)_{\max}$, the following relationship has been proposed:¹⁷

$$(\lambda_b)_{\max} = (\rho/\nu Z M_0)^{1/2} \tag{7}$$

where ρ and M_0 stand for the density and the monomeric molecular weight

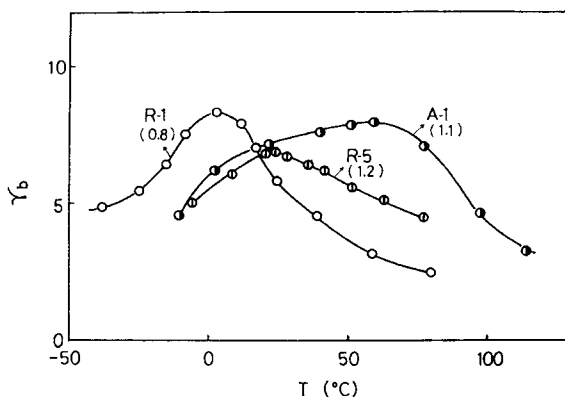


Fig. 18. Temperature dependence of strain at break, γ_b . Number in parenthesis is crosslink density (10^{-4} mole/cc).

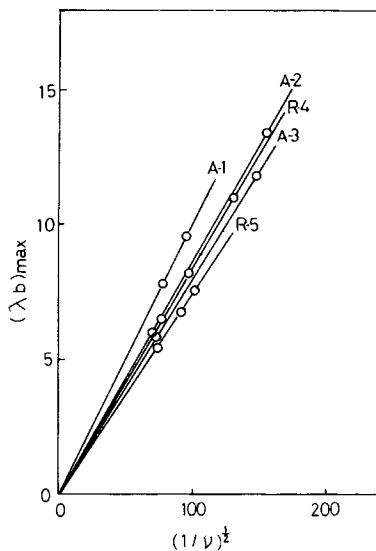


Fig. 19. Dependence of ultimate extension ratio on crosslink density.

of the sample, respectively, and Z is a parameter representing the stiffness of the chain. Equation (7) suggests a linear relationship between $(\lambda_b)_{\max}$ and $\nu^{-1/2}$ for each sample, and Figure 20 illustrates the results of the experimental verification of this expectation. The Z values estimated therefrom for those samples are listed in Table III. These values are in good agreement with those estimated optically for peroxide-cured vulcanizates of the same copolymers.⁴ In Figure 21, the values of Z and $(\lambda_b)_{\max}$ are plotted against the run number for four equimolar copolymers. The chain stiffness increases with the degree of alternation.

It was found previously that in most cases T_{\max} decreases linearly with the crosslink density ν . The same is found in Figure 22 of this study. Extrapolating each straight line to the ordinate, the value of

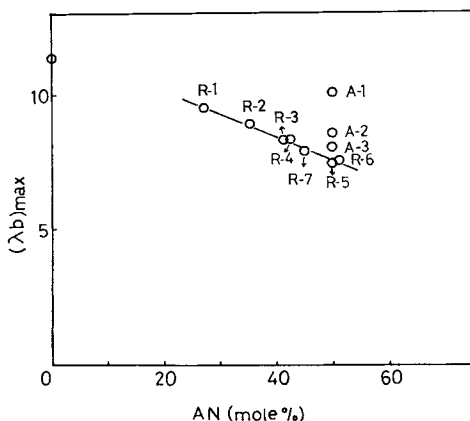


Fig. 20. Dependence of ultimate extension ratio on AN content at crosslink density of 1.0×10^{-4} mole/cc.

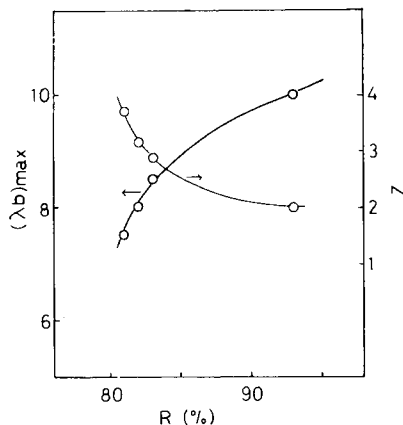


Fig. 21. Dependence of ultimate extension ratio and chain stiffness on run number for equimolar copolymers at crosslink density of 1.0×10^{-4} mole/cc.

TABLE III
Stiffness of Chain, Z and $Z \cdot l$, for Acrylonitrile-Butadiene Copolymers^a

Sample no.	Z	$Z \cdot l, \text{\AA}$
R-1	2.1	8.7
R-2	2.4	9.4
R-3	2.9	11.0
R-4	2.9	11.0
R-5	3.7	13.3
R-6	3.6	13.0
R-7	3.3	12.4
A-1	2.0	7.2
A-2	2.8	9.7
A-3	3.2	11.5

^a Z is the number of monomeric units in a statistical segment; $Z \cdot l$ is the length of the segment in angstrom units.

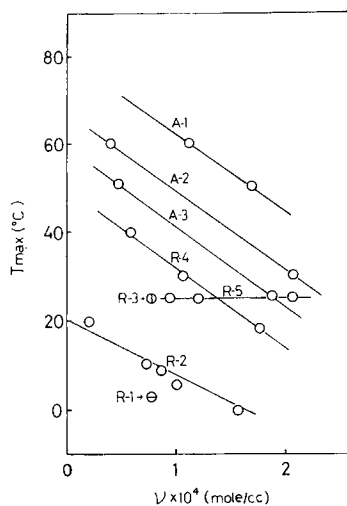


Fig. 22. Dependence of T_{\max} on crosslink density.

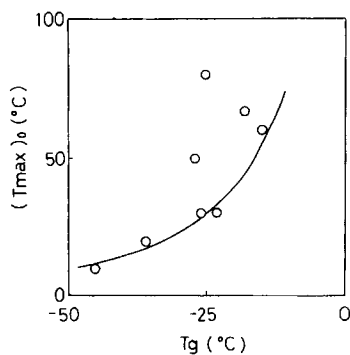


Fig. 23. Reduced T_{\max} vs. T_g .

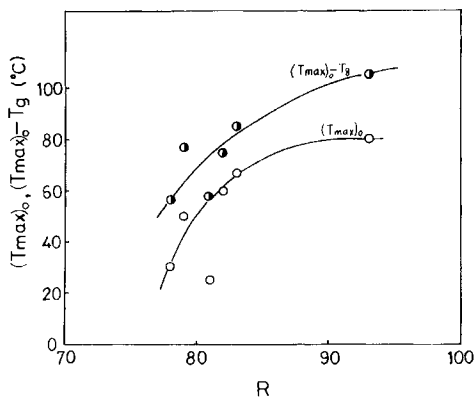


Fig. 24. Reduced T_{\max} and $(T_{\max} - T_g)$ vs. run number.

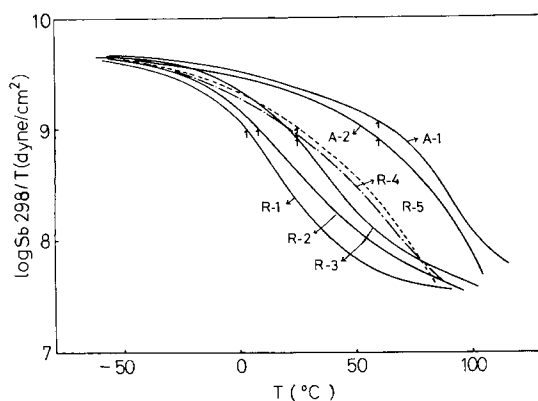


Fig. 25. Temperature dependence of true stress at break at crosslink density of about 1.0×10^{-4} mole/cc.

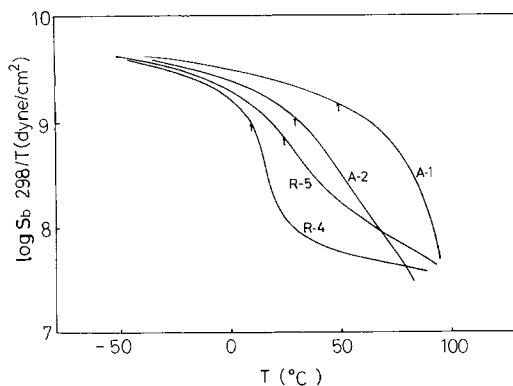


Fig. 26. Temperature dependence of true stress at break at crosslink density of about 2.0×10^{-4} mole/cc.

$(T_{\max})_0$ is obtained. Fujimoto and others²¹ have reported that the differences between $(T_{\max})_0$ and T_θ were kept almost constant in a series of random copolymers (SBR) irrespective of composition. As illustrated in Figure 23, this is not the case in this study, and $(T_{\max})_0$ is not a simple function of T_θ . In Figure 24, $(T_{\max})_0$ and $(T_{\max})_0 - T_\theta$ are plotted against the run number. It was found that $(T_{\max})_0$ increases also with increasing regularity in alternation. In this respect, we may analogously quote the fact that $(T_{\max})_0$ is shifted higher when the *cis* content becomes close to 100% in either polybutadiene or polyisoprene.¹⁸

Figures 25 and 26 illustrate the temperature dependence of the true stress at break of the samples with similar crosslink densities. The arrow in the figures indicates T_{\max} for each sample, and thus, as pointed out before,¹⁹ it may be said that a relatively high level of S_b is generally kept below T_{\max} for each sample in the temperature region.

Summarizing what has been mentioned herein, it may be concluded that the degree of alternation in binary copolymers would have significant effects on T_g , on $(\lambda_b)_{\max}$, and on T_{\max} .

We wish to acknowledge the contributions of Dr. Y. Iseda of Bridgestone Tire Co. and Drs. M. Ichikawa and Y. Takeuchi of Japan Synthetic Rubber Co. for the preparation of copolymers used in this study. The assistance of Mr. Y. Kato and other members of the Evaluation Division of Japan Synthetic Rubber Co. in carrying out a large part of the experimental work is gratefully acknowledged. We would like also to acknowledge the suggestions and discussions of Drs. K. Ninomiya and G. Yasuda, Mr. C. Tosaki, and Mr. M. Kawashima.

References

1. J. Furukawa and Y. Iseda, *J. Polym. Sci. B*, **7**, 47 (1969).
2. J. Furukawa, Y. Iseda, K. Haga, and N. Kataoka, *J. Polym. Sci. A-1*, **8**, 1147 (1970).
3. J. Furukawa, Y. Iseda, K. Haga, N. Kataoka, T. Yoshimoto, T. Imamura, Y. Shido, A. Miyagi, K. Tanaka, and K. Sakamoto, *J. Polym. Sci. B*, **7**, 561 (1969).
4. J. Furukawa, A. Nishioka, and T. Kotani, *J. Polym. Sci. B*, **8**, 25 (1970).
5. J. Furukawa and A. Nishioka, to be published.
6. G. Yasuda and K. Ninomiya, *Nippon Gomu Kyokaishi*, **39**, 81 (1966).
7. C. Tosaki, to be published.
8. M. Mooney, *J. Appl. Phys.*, **11**, 528 (1940).
9. R. S. Rivlin, *Rheology*. Vol. I, Academic Press, New York, 1956, p. 351.
10. E. Maekawa, S. Yanagisawa, S. Kusamizu, and K. Ninomiya, *Nippon Gomu Kyokaishi*, **41**, 753 (1968).
11. K. Fujino, I. Furuta, S. Kawabata, and H. Kawai, *Zairyo*, **13**, 404 (1964).
12. K. Ninomiya and G. Yasuda, *Rubber Chem. Technol.*, **42**, 714 (1969).
13. P. J. Flory and J. Rehner, *J. Chem. Phys.*, **11**, 521 (1943).
14. P. J. Flory, *J. Chem. Phys.*, **18**, 108 (1950).
15. J. D. Ferry, *Viscoelastic Properties of Polymers*, Wiley, New York, 1961.
16. K. Ninomiya and I. Furuta, *Rubber J.*, **152**, 33 (Aug. 1970).
17. J. Furukawa, S. Yamashita, T. Kotani, and M. Kawashima, *J. Appl. Polym. Sci.*, **13**, 2527 (1969).
18. S. Kusamizu, unpublished data.
19. S. Kusamizu, K. Ninomiya, and Y. Hirose, *Nippon Gomu Kyokaishi*, **43**, 385 (1970).
20. K. Fujimoto, T. Migita, and T. Kasuya, *Nippon Gomu Kyokaishi*, **42**, 411 (1969).

Received November 23, 1970

Revised February 26, 1971